J Headache Pain (2000) 2:67–71

ENRICO GREPPI AWARD PAPER

Vijaya Nagesh
Michael Welch
Sheena K. Aurora
Neil Gelman
Shanthi Gopal

Is there a brainstem generator of chronic daily headache?

V. Nagesh (✉) • S.K. Aurora
N. Gelman • S. Gopal
NMR/Neurology Research,
E & R Basement,
Department of Neurology,
Henry Ford Hospital,
2799 West Grand Boulevard,
Detroit, MI 48202-2689, USA
E-mail: vijaya@neurnis.neuro.hfh.edu
Tel.: +1-313-916-2620
Fax: +1-313-916-1324

M. Welch
University of Kansas Medical Center,
Kansas City, Kansas, USA

Abstract Using BOLD-fMRI we have previously documented activation of the red nucleus (RN) and substantia nigra (SN) during spontaneously and visually activated migraine headaches. These observations prompted us to study brainstem function in chronic daily headache patients using high-resolution magnetic resonance imaging (MRI) techniques. Seventeen chronic daily headache (CDH) patients, ten episodic migraine (EM) patients and fifteen controls (N) were imaged with a 3 tesla MRI system. For each subject, the relaxation rates R2, R2* and R2' were obtained for RN and SN. There was a significant decrease in R2' and R2* values for RN and SN in CDH compared to N and EM groups ($p < 0.05$), but no significant difference between the N and EM groups. A decrease in R2' and $R2^*$ indicates reduced deoxyhemoglobin and hence persistent activation of the RN and SN in CDH patients most likely secondary to ongoing headache at the time of study. The imaging data provide objective evidence of disturbed central nervous system function in CDH.

Key words Chronic daily headache • Migraine • Magnetic resonance imaging • Red nucleus • Substantia nigra • Image processing

Introduction

The mechanisms of chronic or persistent daily headache (CDH) that evolves from episodic migraine remain to be determined and have been studied rarely. During episodic migraine, activation occurs in brainstem structures involved in nociception [1–4]. For example, in positron emission tomography (PET) studies during spontaneous migraine without aura, increased blood flow was measured in mesencephalic regions that possibly reflected dorsal raphe nuclei (DRN), periaqueductal gray matter (PAG) and locus ceruleus (LC) activation [5]. Using blood oxygen level dependent (BOLD) functional magnetic resonance imaging (fMRI) we have recently observed activation of the red nucleus (RN) and substantia nigra (SN) during spontaneous [6] and visually activated attacks of migraine with and without aura [7]. The reasons for RN and SN activity in migraine attacks remain to be established but both structures have been implicated in nociception and autonomic dysfunction.

The above observations prompted a study of brainstem function in CDH. We used high-resolution MR techniques to map the transverse relaxation rates R2 (1/T2), R2* (1/T2*) and R2' (R2* - R2) in brain and, in particular, in the RN and SN. These measures are sensitive to shifts in the paramagnetic properties of free iron in brain tissue and blood. We report decreased R2' and R2* in the RN and SN as evidence for persistent activation of brainstem structures in CDH. To the best of our knowledge, this is the first report of disturbed central nervous system (CNS) function in chronic daily headache.

Subjects and methods

Three groups of subjects were imaged (Table 1). The institutional review board of Henry Ford Health Sciences Center approved the imaging protocol. All subjects who participated in this study provided written informed consent prior to the study. The first group comprised 17 patients diagnosed with chronic daily headache (CDH) preceded by episodic migraine without aura attacks; there were 3 men and 14 women aged 22-57 years (mean age ± SD, 38 ± 11 years). In the second group 10 patients with episodic migraine without aura (EM), 2 males and 8 females aged 23-53 years (mean age ± SD, 36 ± 10 years) were imaged. The third group studied consisted of 15 healthy normal adults (N), 5 men and 10 women aged 20-64 years (mean age ± SD, 38 ± 12 years). The difference in the mean age of the three groups was not statistically significant ($p = 0.83$, repeated measure ANOVA, Table 1) nor were the gender differences ($p = 0.55$). International Headache Society (IHS) classification guidelines [8] were used to evaluate and diagnose CDH and EM patients. No migrainous feature was present in any of the EM patients at MRI.

Imaging techniques

All MR images were acquired with a 3 tesla, 80-cm (inner diameter) magnet (Magnex Scientific, Abingdon, England) with a maximum gradient strength of 18 mT/m and 250 µs ramp time. A quadrature birdcage head coil was used for imaging. Spin-echo sagittal images were obtained to align the imaging plane so that it was parallel to the plane encompassing both the inferior colliculus and mammillary body.

Multislice measurements of R2, R2' and R2* were performed in a single acquisition using the gradient-echo sampling of free induction decay and echo (GESFIDE) sequence [9]. The timing of the echoes in this sequence was identical to that used previously [10]. Briefly, two slice-selective 90º and 180º radiofrequency (RF) pulses were used in this sequence. Five gradient echoes were acquired between the 90º and 180º RF pulses, followed by acquisition of six echoes after the 180º pulse. The final (eleventh) echo produced a spin-echo at 98 ms. Twenty-four thin contiguous 2.2-mm slices from the ponto-medullary border to slightly above the superior border of the putamen were obtained within 10.7 min. A 128x128 imaging matrix with a 220-mm field of view, and 2500 ms repetition time was used for image acquisition. Even and odd slices were obtained in separate scans to avoid interference from adjacent slices. The imaging time of the entire protocol, inclusive of positioning and shimming was approximately 20 min.

Table 1 Demographics of control (N) subjects, patients with chronic daily headache (CDH) and patients with episodic migraine (EM) studied with MRI to measure transverse relaxation rates of brainstem structures. The difference in the mean age of the three groups studied was not statistically significant ($p = 0.89$, repeated measure ANOVA)

	N (n = 15)	CDH (n = 17)	EM (n = 10)
Mean age ± SD, years	38±12	38±11	36±10
Age range, years	20–64	22–57	23–53
Females, n	10	14	8
Males, n	5	3	2

Image analysis

The image sets were Fourier transformed and zero-filled to yield 256x256 in-plane images for each of the 264 two-dimensional images (24 slices x 11 echoes). Maps of R2, R2' and R2* were obtained as described in a previous study [9]. The procedure involved construction of R2* maps from the first 5 echoes and $R2^-$ (= R2–R2') maps from the last six echoes of the GESFIDE sequence [10]. Further, the R2* and $R2^-$ maps were converted to R2 and R2' maps using the following expressions:

$$R2 = (R2^* + R2^-)/2$$

$$R2' = (R2^* - R2^-)/2$$

Brain tissue segmentation was performed using the iterative self-organizing data analysis technique clustering technique (ISODATA) [11]. ISODATA is a semi-automated algorithm based on techniques of multivariate statistical analysis. The algorithm is based on the Euclidean measures of pattern similarity. A vector feature is constructed at each spatial location from the set of input data. The clusters are determined in such a way that the intra-set distance in each cluster is kept to a minimum, and the inter-set distance between two clusters is made as large as possible. The number of source images determines the dimension of the Euclidean (feature) space in which the clustering is carried out. To potentially improve tissue specificity, qualitatively different images are used to increase the likelihood of separating two tissues with similar signature profiles.

For each subject, all image slices reconstructed from the final echo (TE/TR = 98/2500 ms) of the GESFIDE sequence were reviewed visually to identify and localize slices containing the periaqueductal gray matter (PAG), red nucleus (RN), and substantia nigra (SN). The PAG, RN and SN were visible in two or more slices for all cases reported in this study. ISODATA segmentation was used to accurately delineate and identify the entire volume of the RN and SN. Eleven images (one from each echo of GESFIDE sequence) were used as source images for the ISODATA segmentation of each slice. This technique ensured that anatomic borders were not crossed. An operator classified the resulting zones into gray matter, white matter, cerebrospinal fluid (CSF), PAG, RN and SN. For each subject, the R2 (1/T2), R2* (1/ T2*) and R2' (1/T2*–1/T2) relaxation rates of the RN, SN and PAG were obtained for the left and right hemispheres separately by projecting the corresponding segmented zones onto the maps. Measurements derived from multiple slices for each subject were expressed as a weighted average.

Statistical analysis

The relaxation rates, R2, R2' and R2* of RN and SN for each subject are presented as mean ± SD. One way analysis of variance (ANOVA) was used to test the null hypothesis of equality of population means among the three groups. The significance level was set at $p < 0.05$. Student's paired t test was used to compare the relaxation rates for the right versus left hemispheres.

Results

Representative images containing the PAG, RN or SN of one subject are shown in Fig. 1. The RN and SN are readily identified as hypointense regions and the PAG is adjacent to the cerebral aqueduct (hyperintense area). ISODATA segmentation and classification of the different zones are illustrated in Fig. 2. Representative maps of R2, R2' and R2* for a section through the midbrain are shown in Fig. 3. The mean ± SD of R2, R2' and R2* obtained for the RN and SN of the left and right hemispheres for the N, CDH and EM groups are presented in Table 2.

There was a significant decrease in R2' and R2* values of the RN and SN of CDH patients compared to N and EM groups ($p < 0.05$), but there was no significant difference in the relaxation rates of either the SN or RN between the N and EM groups. The R2 values among the three groups in both the RN and SN were not significantly different. Similar results were observed for both left and right hemispheres. In addition, no intragroup hemispheric differences were noted in the relaxation rates of either the RN or SN using Student's paired *t* test. Results from the PAG analysis form the subject of a separate communication.

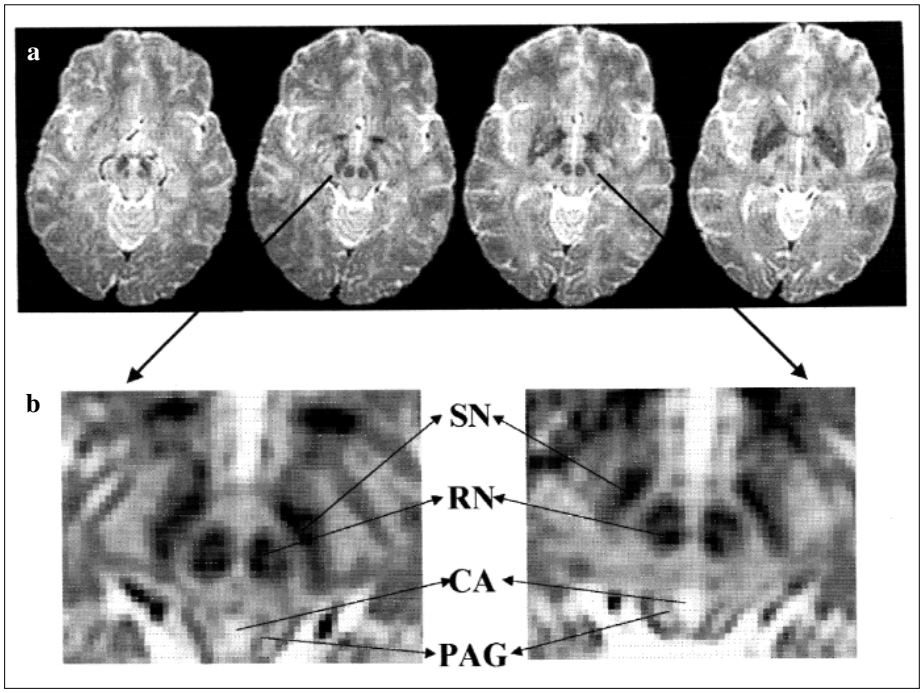

Fig. 1 a Spin-echo MR images (echo time/repetition time (TE/TR) = 98/2500 ms) of four contiguous 2.2-mm slices obtained with the gradient-echo sampling of free induction decay and echo (GESFIDE) sequence. **b** Magnified views of the center two images of **a**. Arrows pointing to the hypointense areas correspond to the substantia nigra (*SN*) and the red nucleus (*RN*). The hyperintense area corresponding to *CA* is the cerebral aqueduct, and surrounding *CA* is the periaqueductal gray matter (*PAG*)

Table 2 The transverse relaxation rates R2, R2' and R2* of the red nucleus (RN) and substantia nigra (SN), expressed as mean ± standard deviation for control (N), chronic daily headache (CDH) and episodic migraine (EM) groups. Differences in the relaxation rates among the three groups were tested using one way analysis of variance (ANOVA), with significance level set at $p < 0.05$. There is a significant decrease in the R2' and R2* values of RN and SN of CDH patients compared to the N and EM groups.

	Red nucleus			Substantia nigra		
Relaxation rate (1/ms)	N	CDH	EM	N	CDH	EM
R2-Right	24.67 ± 1.69	23.75 ± 1.91	24.34 ± 1.55	27.06 ± 2.29	26.33 ± 2.66	28.25 ± 2.07
R2-Left	24.90 ± 1.82	23.48 ± 1.92	25.58 ± 1.65	26.20 ± 2.24	25.74 ± 2.62	27.60 ± 2.19
R2'-Right	14.93 ± 2.14	10.75 ± 2.27	13.89 ± 1.82	15.03 ± 3.31	11.30 ± 3.32	15.75 ± 3.20
R2'-Left	13.78 ± 2.20	10.69 ± 1.97	14.07 ± 1.87	14.39 ± 3.42	11.80 ± 3.30	15.82 ± 2.84
R2*-Right	39.62 ± 2.47	34.44 ± 2.85	38.46 ± 2.06	42.76 ± 3.97	35.34 ± 4.21	44.02 ± 3.80
R2*-Left	38.88 ± 2.41	34.01 ± 2.61	39.50 ± 2.35	41.33 ± 3.93	37.74 ± 3.78	43.41 ± 3.53

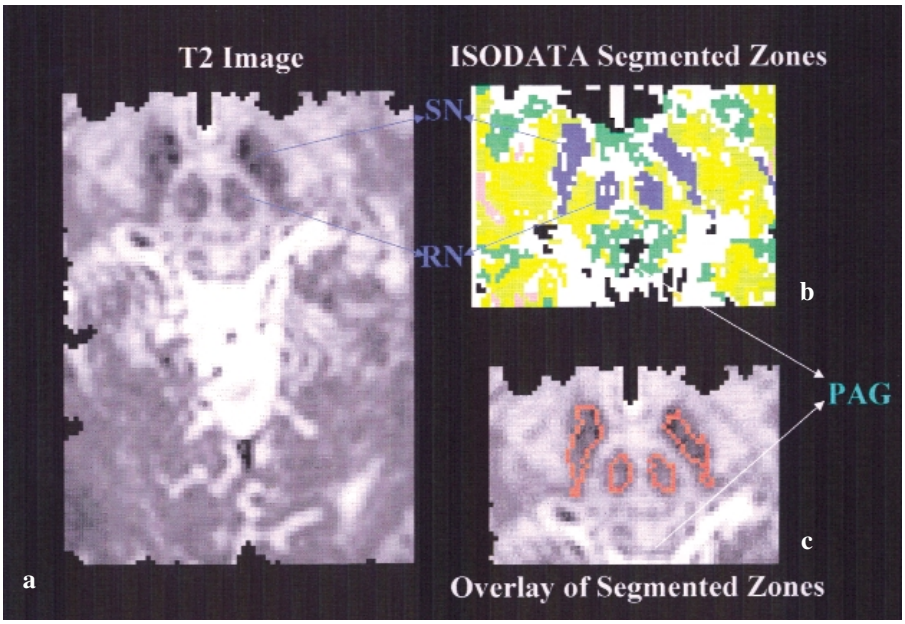

Fig. 2 a Spin-echo T2-weighted image (TE/TR = 98/2500 ms) of the midbrain showing the red nucleus (*RN*) and substantia nigra (*SN*). Eleven images, one from each echo of the GESFIDE pulse sequence were used in the computer cluster analysis (ISODATA) to segment brain tissue. **b, c** Results of ISODATA segmentation (b) and the segmented zones superimposed on the T2 image (enlarged view) (c). Each color of the ISODATA segmented image is representative of a different cluster with unique properties in feature space.

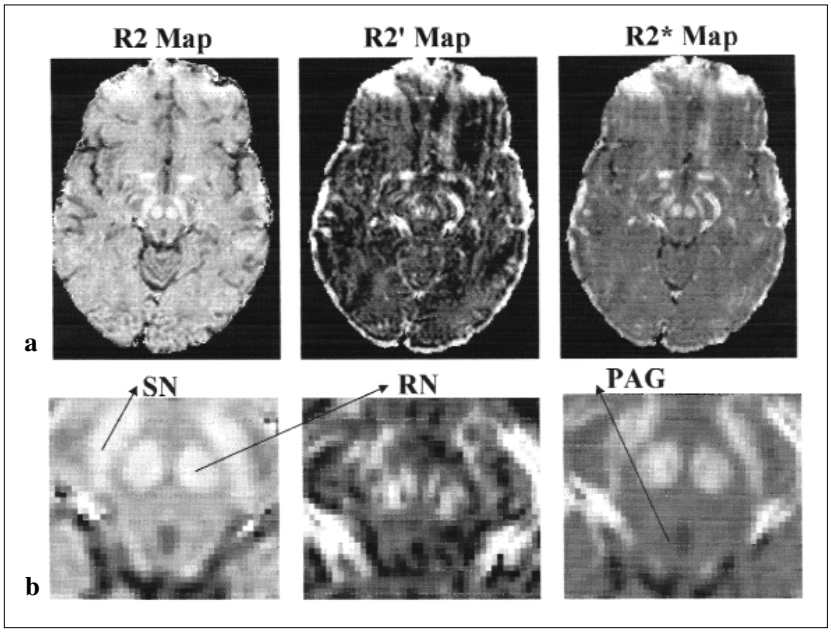

Fig. 3 a Transverse relaxation rates, R2, R2' and R2* maps of a single 2.2-mm slice. Image reconstruction and calculation of these maps is detailed in the text. **b** Enlarged views of the corresponding map detailing the brainstem structures that were studied. The red nucleus (*RN*) and substantia nigra (*SN*) appear hyperintense on the three relaxation rate maps. *PAG*, periaqueductal gray matter

Discussion

Using high-resolution MRI techniques, we have mapped transverse relaxation rates R2, R2' and R2* in patients with chronic daily headache and compared them to healthy control subjects and episodic migraine patients. Increased R2 and R2', especially the latter, is more specific to deposition of non-heme iron in tissues [10]. A decrease in these measures reflects the influence of free iron from deoxyhemoglobin.

There was no alteration of R2 in any of our subject groups, providing important structural evidence of no change in tissue water content. The decreases in R2' and R2* of RN and SN in the CDH patient group are explained best by flow activation and hyperoxia of these structures associated with head pain. This is supported by unchanged R2' and R2* in episodic migraine patients without headache. A study of CDH patients when headache-free is needed to evaluate if there is increased tissue iron in RN and SN. As noted in the Introduction, activation of these brainstem structures has been observed using fMRI-BOLD [6, 7]. The

precise reasons for activation of RN and SN in migraine attacks remain to be established but could include both nociceptive and autonomic dysfunctions.

These imaging data provide the first objective evidence of disturbed CNS function in CDH. Although we did not study cortical function, the absence of aura symptoms in this condition supports the possibility of a brainstem generator for head pain, similar to that suggested for episodic migraine without aura [5]. Because different brain regions were studied, firm comparative conclusions cannot be drawn between the latter report and our own. Nevertheless, persistent activation of other components of the brainstem nociceptive system, such as the trigeminal nucleus, can be inferred from both studies.

In conclusion, we have shown persistent activation of the red nucleus and substantia nigra in migraine without aura patients with episodic headache that over time becomes daily and persistent. We offer this as preliminary evidence for a brainstem generator of chronic daily headache.

Acknowledgements This work was supported by NIH Grant number P50-NS32399.

References

1. Raskin NH, Hosobuchi Y, Lamb S (1987) Is the brain pain-insensitive? Cephalalgia 7[Suppl 6]:23–25
2. Moskowitz MA (1984) The neurobiology of vascular head pain. Ann Neurol 16:157–168
3. Lance JW (1990) A concept of migraine and the search for the ideal headache drug. Headache 30[Suppl 1]:17–28
4. Goadsby PJ, Edvinsson L, Ekman R (1988) Release of vasoactive peptides in the extracerebral circulation of humans and the cat during activation of the trigeminovascular system. Ann Neurol 23:193–196
5. Weiller C, May A, Limmroth V, Juptner M, Kaube H, Schayk RV, Coenen HH, Diener HC (1995) Brainstem activation in spontaneous human migraine attacks. Nat Med 1:658–660
6. Welch KMA, Cao Y, Aurora SK, Wiggins G, Vikingstad EM (1998) MRI of the occipital cortex, red nucleus, and substantia nigra during visual aura of migraine. Neurology 51:1465–1469
7. Cao Y, Aurora SK, Vikingstad EM, Patel SC, Welch KMA (1999) Functional MRI of the red nucleus and occipital cortex during visual stimulation of subjects with migraine. Cephalalgia 19:462 (abstract)
8. Headache Classification Committee of the International Headache Society (1988) Classification and diagnostic criteria for headache disorders, cranial neuralgias and facial pain. Cephalalgia 8 [Suppl 7]:1–96
9. Ma J, Wehrli FE (1996) Method for image-based measurement of the reversible and irreversible contribution to the transverse relaxation rate. J Magn Reson B 111:61–69
10. Gelman N, Gorell JM, Barker PB, Savage RM, Spickler EM, Windham JP, Knight RA (1999) MR imaging of human brain at 3.0 T: preliminary report of transverse relaxation rates and relation to estimated iron content. Radiology 210:759–767
11. Bezdek JC (1980) A convergence theorem for the fuzzy ISODATA clustering algorithm. IEEE Trans Pattern Anal Mach Intell PAMI-2 1:1–8